

# TIME DEPENDENT STUDY FOR AN X-RAY FEL OSCILLATOR AT LCLS-II

J. Zemella<sup>1,2</sup>, W. M. Fawley<sup>1</sup>, R. R. Lindberg<sup>3</sup>, and T. J. Maxwell<sup>1</sup>

<sup>1</sup>DESY, Hamburg, Germany

<sup>2</sup>SLAC, Menlo Park CA, USA

<sup>3</sup>ANL, Argonne IL, USA

## Abstract

The LCLS-II with its high repetition rate and high quality beam will be capable of driving an X-ray free electron laser oscillator at higher harmonics in the hard X-ray regime (0.1 nm). The oscillator consists of a low loss X-ray crystal cavity using diamond Bragg crystals with meV bandwidth. The expected average spectral flux has been estimated to be at least two orders of magnitude greater than present synchrotron-based sources with highly stable, coherent pulses of duration 1 ps or less for applications in Mössbauer spectroscopy and inelastic x-ray scattering. A more detailed study of the start up of a fifth-harmonic X-ray FEL oscillator at LCLS-II will be presented with full, time-dependent simulations.

## INTRODUCTION

The planned LCLS-II cryogenic linac based on TESLA technology [1, 2] at SLAC will be operated in ‘cw-mode’ with a repetition rate of 0.929 MHz. This enables one to develop new concepts for generating hard X-rays including low-gain FEL schemes such as X-ray free electron laser oscillators (XFELO) based on a high reflectivity crystal cavity with narrow bandwidth in the order of 10 meV [3]. The advantages of an XFELO are the full coherence and spectral purity of the X-ray pulse compared to state of the art sources like SASE (self amplified spontaneous emission) FELs (LCLS-I [4], SACLA [5]) based on a stochastic process leading to fluctuating pulse properties. Self seeding technique is able to improve longitudinal coherence in hard X-ray [6] but not reaching full, stable longitudinal coherence and typically include a broad SASE background that may complicate, e.g., precision inelastic X-ray scattering (IXS) experiments.

The design beam energy of the LCLS-II cryogenic linac is 4 GeV. To generate Ångstrom wavelengths one can instead amplify a higher harmonic of the FEL pulse [7]. We consider in this paper the fifth harmonic at 14.4 keV using the Bragg reflection of Diamond (hkl)=(733) where (hkl) are the Miller indices.

We present progress on the feasibility study started last year where initial performance estimates were presented in [8]. This paper is focused on verifying the startup process of the XFELO and saturation pulse properties using the time-dependent simulation code Ginger [9] in oscillator mode, extended to simulate higher harmonics.

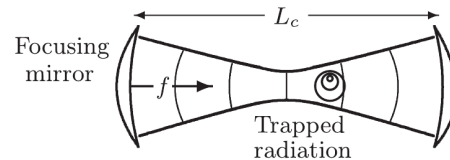


Figure 1: Used cavity design used in Ginger simulations.

## LAYOUT

The cavity model used in simulations is depicted in Fig. 1. Two focusing elements define the waist  $\omega_0$  inside the undulator which can be expressed by the Rayleigh length  $Z_R$  and the wavelength  $\lambda$

$$Z_R = \frac{\pi\omega_0^2}{\lambda}, \quad (1)$$

$$f = \frac{L_c}{4} + \frac{Z_R^2}{L_c}, \quad (2)$$

with cavity length  $L_c$  and focal strength  $f$  of the mirrors. Spectral filtering from the Bragg reflectors is done by applying the wavelength-dependent complex reflectivity of the two Bragg crystals, one thick (high-reflectivity) and one thin (extraction mirror) crystal. The path length change induced by Bragg reflection leading to cavity length detuning is compensated here by multiplying the complex reflectivity with the proper group delay phase factor as described in [10]. The assumed crystal reflectivity of both Bragg C\*(733) crystals is shown in Fig. 2. For the present study the modified cavity design shown in Fig. 1 is a modification of the tunable, four crystal, zig-zag cavity scheme previously discussed. However, for gain studies only matched mode size, Rayleigh length, and electron beam beta function in the undulator must be matched which can be achieved by the cavity described. Of course this may change with a more precise description of the 3D angular divergence which is not addressed here.

## SIMULATIONS

For simulating an XFELO for LCLS-II a 167 fs long Gaussian current profile with 120 A peak current and 200 keV Gaussian energy spread is assumed. Further parameters are gathered in Table 1.

Some optimization steps were performed for optimizing FEL gain. The first step is to find the right energy detuning, shown in the scan of Fig. 3 to maximize gain in steady state.

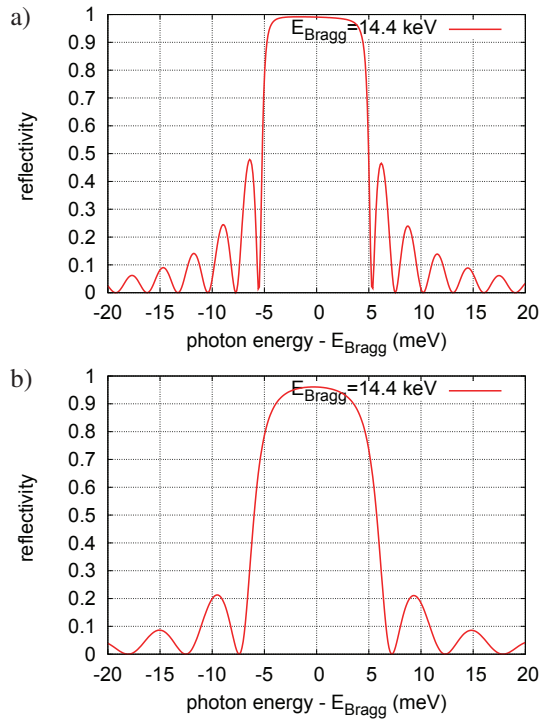


Figure 2: a) Reflectivity of a diamond crystal using Bragg reflex (733) with 200 micron thickness. b) Reflectivity of a diamond crystal using Bragg reflex (733) with 107 micron thickness. Transmission of crystal is about 4 %.

Table 1: Electron Beam and Cavity Parameters

Parameter	Value	Units
e <sup>-</sup> -beam energy	4.0	GeV
Peak current	120.0	A
Bunch charge	50.0	pC
Bunch length (rms)	166.7	fs
Energy spread	200.0	keV
Norm. emittance	0.3	μm
Photon energy at 5 <sup>th</sup> harmonic	14.4	keV
Undulator period	26.0	mm
Number of undulator periods	1250	
Undulator parameter K	1.433	
loss per round-trip	15.0	%
Rayleigh length	12.0	m
Distance rad. waist-undulator center	-1.0	m

The proper phase shift to compensate the exact cavity path length is done by several simulation runs. To obtain the maximum gain versus beta function at undulator center and the corresponding Rayleigh length of the light in the undulator a scan of both quantities was also performed. The last step is a scan of the undulator center/electron beam waist and the radiation waist position. A 1 m upstream shift of the undulator center with respect to the cavity center optimizes the gain, though this dependence is quite weak.

After these optimizations, we find the following. The

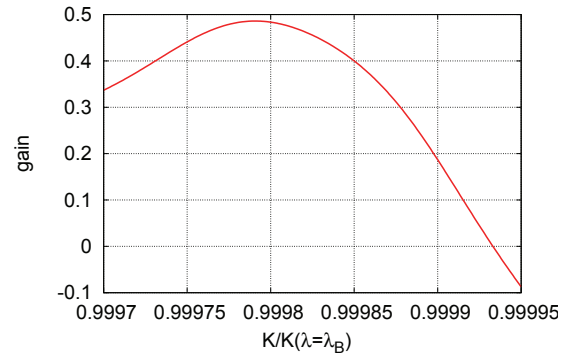


Figure 3: Single pass gain in dependence of the undulator parameter.  $K(\lambda = \lambda_B)$  is the undulator parameter for the center wavelength of Bragg reflection.

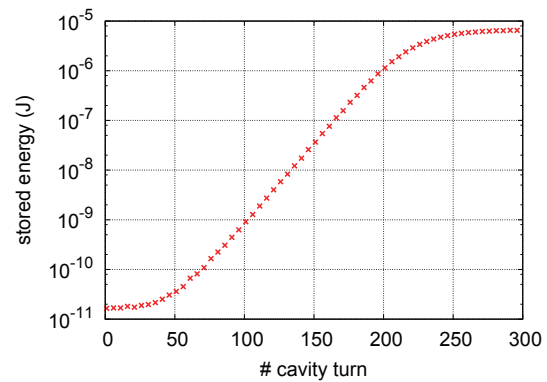


Figure 4: Evolution of the pulse energy for number of cavity round-trips.

photon pulse energy dependence on cavity round-trip number is shown in Fig. 4. The intra-cavity saturation power is  $E_{Sat} = 6.6 \mu\text{J}$  after 275 cavity passes. Per-pass gain becomes exponential after just 50 passes. The net gain per pass is 7.6 % (including the 15 % loss per turn). This is noticeably less than the single-pass gain indicated by previous steady state estimates. The decrease of the gain is explained by the short bunch duration and much narrower actual crystal bandwidth which in this case are not a near-optimal Fourier limit pair. This leads to a reduced overlap between electrons and photons and therefore to a smaller gain. We find (not shown) that when increasing bunch length to 400 fs (rms) gain is a factor 2.5 higher and peak power is increased to 40 MW for a combined factor of 5 greater flux than in the present comparison. However in this case, the charge is necessarily increased to 120 pC to maintain sufficient peak current.

The pulse profile and spectrum are shown in Fig. 5. The temporal pulse profile is with 205 fs (rms) longer than the electron bunch length of 167 fs (rms). There are trailing pulses which are a result of the wavelength-dependent crystal reflectivity. The spectral width of 5 meV is slightly narrower than the reflectivity bandwidth of the crystals.

The photon pulse parameters are listed in Table 2.

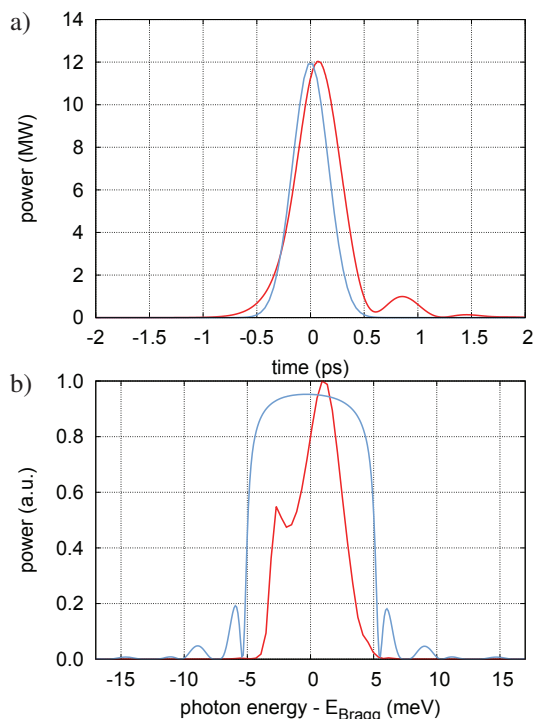


Figure 5: a) Temporal pulse profile at saturation in red. The current profile is also drawn in blue without y scaling. b) Spectral pulse profile at saturation in red. The combined crystal reflectivity of the thick and the thin crystal is also drawn in blue.

Table 2: Intra Cavity Photon Pulse Parameters

Parameter	Value	Units
Net gain per cavity pass	7.6	%
Applied loss per cavity pass	15.0	%
FEL gain per cavity pass	22.6	%
Pulse length at saturation (rms)	205.0	fs
Pulse bandwidth at saturation	5.0	meV
Pass number to saturation	250	
Intra-cavity pulse energy at saturation	6.6	μJ
Out-couple ratio	4.0	%
Output photons per pulse	$1.1 \cdot 10^8$	
Output spectral flux (~2 MHz rep. rate)	$4.2 \cdot 10^{13}$	ph/s/meV

## CONCLUSION

An XFEL driven by the LCLS-II superconducting linac at 5<sup>th</sup> harmonic photon energies of 14.4 keV using 50 pC

bunches leads to a high brightness source which is able to improve achievable spectral flux by orders of magnitude for applications such as IXS and X-ray photon correlation spectroscopy, hungry for high coherence X-rays in a very narrow bandwidth. The time-dependent simulation with ideal Gaussian bunch shape leads to promising results in reasonable agreement to initial estimates while suggesting design modification to reach desired performance goals in the  $10^{14}$  ph./s/meV range. Due to beam power limitations bunch lengthening is not suitable solution but would help to improve electron bunch - photon pulse overlap. A different Bragg reflex with a larger bandwidth shall increase the overlap the same manner helping to improve the performance of an XFEL at LCLS-II. With this benchmarking complete, further optimization and numerical studies will now be further extended to include the more realistic start to end-simulated electron bunches to investigate gain degradation from sub-optimal longitudinal phase space distributions.

## REFERENCES

- [1] SLAC National Accelerator Laboratory, Linac Coherent Light Source II Conceptual Design Report, No. SLAC-R-978 (2011).
- [2] B. Aune et al., "Superconducting TESLA cavities", Phys. Rev. ST Accel. Beams **3**, 092001 (2000).
- [3] K.-J. Kim, Y. Shvyd'ko, and S. Reiche, "A Proposal for an X-Ray Free-Electron Laser Oscillator with an Energy-Recovery Linac", Phys. Rev. Lett. **100**, 244802 (2008).
- [4] P. Emma et al., First lasing and operation of an ångstrom-wavelength free-electron laser", Nature Photonics **4**, 641 (2010).
- [5] T. Ishikawa et al., "A compact X-ray free-electron laser emitting in the sub-ångstrom region", Nature Photonics **6**, 540 (2012).
- [6] J. Amann et al., "Demonstration of self-seeding in a hard-X-ray free-electron laser", Nature Photonics **6**, 693 (2012).
- [7] J. Dai, H. Deng, and Z. Dai, "Proposal for an X-Ray Free Electron Laser Oscillator with Intermediate Energy Electron Beam", Phys. Rev. ST Accel. Beams **108**, 034802 (2012).
- [8] T. J. Maxwell et al., "Feasibility study for an X-ray FEL oscillator at the LCLS-II", TUPMA028, 6-th IPAC 2015, Richmond VA, USA.
- [9] W. M. Fawley, "A User Manual for GINGER-H and its Post-Processor XPLOTGINH", Version 2.0k, June 2012.
- [10] R.R. Lindberg et al., "Performance of the x-ray free-electron laser oscillator with crystal cavity", Phys. Rev. ST Accel. Beams **14**, 010701 (2011).